Photogeneration of Manganese(III) from Luminescent Manganese(II) Complexes with Thiacalixarene Ligands: Synthesis, Structures and Photophysical Properties

Niall O'Toole, Constance Lecourt, Yan Suffren, Andreas Hauser, Lhoussain Khrouz, Erwann Jeanneau, Arnaud Brioude, Dominique Luneau, Cédric Desroches

Photo-generation of manganese(III) from luminescent manganese(II) complexes with thiacalixarene ligands: synthesis, structures and photo-physical properties.

Niall O'Toole,[a] Constance Lecourt, [a] Yan Suffren,[b], [c] Andreas Hauser,[b] Lhoussain Khrouz [d], Erwann Jeanneau [a], Arnaud Brioude [a], Dominique Luneau [a], Cédric Desroches.*[a]

[a] *Laboratoire des Multimatériaux et Interfaces (UMR 5615), Université Claude Bernard de Lyon 1, Campus de la Doua, 69622 Villeurbanne, France.*

E-mail: cedric.desroches@univ-lyon1.fr

[b] *Département de chimie physique, Université de Genève, 30 Quai Ernest-Ansermet, 1211 Genève 4, Switzerland.*

[c] *Univ Rennes, INSA Rennes, CNRS, ISCR "Institut des Sciences Chimiques de Rennes", F-35000 Rennes, France.*

[d] *Laboratoire de chimie (UMR 5182), Ecole normale supérieure (ENS) Lyon, 15 parvis René Descartes, BP 7000, 69342 Lyon Cedex 07, France.*

Abstract

The photo-physical properties of the compound $[(ThiaSO_2)(Mn^{II})_2(DMF)_4(H_2O)_2]$ (2), $ThiaSO_2$ = *p-tert*butylsulphonylcalix[4]arene, are presented and compared to the ones of $[(ThiaSO_2)_2(Mn^{II})_4F]K$ (1). The orange luminescence of 2 is attributed, as for 1, to the Mn^{II} centred $^4T_1 \rightarrow {}^6A_1$ transition and shows, for this type of complex, the weak influence of the

Mn^{2+} coordination and $ThiaSO_2$ conformation on this luminescence, the temperature and pressure dependence and quenching by molecular dioxygen of which are reported for 2. The latter is attributed to energy transfer from the $^4T_1$ state exciting dioxygen to its $^1\Sigma^+_g$ state and is responsible for the photosynthesis of the $[(ThiaSO_2)(Mn^{III})(DMF)_2]Na$ (3) complex in DMF solution from 1 or 2. This reaction was studied by UV-visible and EPR spectroscopy. The molecular structure and EPR spectroscopy of 3 are also presented.

Introduction

Conversion of light energy, especially of solar energy, to chemical or electrical energy represents one of the greatest scientific challenges of the 21st century. A multitude of studies have been directed towards this goal, often using living systems as models.[1] The generation and quenching of excited states by photo-induced electron or energy transfer is a crucial phenomenon in these processes.[1],[2] With the goal of understanding and imitating this type of transformation, numerous transition metal based photo-sensitizers have been conceived. When oxygen is activated by such a molecular system, several photo-oxygenation mechanisms are possible, defined as type I and type II mechanisms, constituting a significant domain of potential applications.[3],[4] Studies until present generally show two different types of photo-sensitizer based on metal complexes to be the most effective: metalloporphyrins and metallopoly(pyridyl) complexes. To our knowledge, no example of a photo-sensitizer complex is known with the family of calixarene ligands.

Recently we discovered the strong luminescence, emitted at approximately 600 nm (excitation at 350 nm) by tetranuclear clusters of Mn^{II} ions and two $ThiaSO_2$ macrocycles ($ThiaSO_2$ = p-tert-butylsulfonylcalixarene) $[(ThiaSO_2)_2(Mn^{II})_4F]K$ (1), induced by the role of $ThiaSO_2$ as an antenna for the sensitization of the Mn^{II} ion.[5],[6] Spectroscopic studies have allowed us to characterize the high sensitivity of the luminescence quenching by energy transfer from the excited complex to O_2 in the solid state as well as in solution. The rarity of

luminescence phenomena for Mn^{II} ions complexes and the extreme sensitivity to oxygen, led us to modify and develop these molecular systems. First, we want to know whether the biprismatic trigonal coordination of the Mn^{II} ion and the conformation of the macrocycle have a significant influence on the luminescence of this molecular system. Secondly, we want to understand their photo-reactivity, which turns the initially colourless DMF solution to purple.

In order to investigate these points, here we report first the results of spectroscopy measurements on the dinuclear compound $(ThiaSO_2)(Mn^{II})_2DMF_4(H_2O)_2$ (2), where the Mn^{2+} ion is found in a distorted octahedral coordination and the $ThiaSO_2$ adopts the 1,2-alternate conformation. We will then present the photo-reactivity studies of both molecular systems 1 and 2 in solution. The effect of irradiation at different wavelengths (360, 400 nm), and the atmosphere under which the reaction is carried out (presence or absence of oxygen), will be discussed. The final products $[ThiaSO_2Mn^{III}(DMF)_2]Na$ (3) and the superoxide ion $O_2^{\bullet-}$ (Scheme 1) from photo-bleaching of 1 and 2 will be isolated and characterized. Finally, a hypothesis for the mechanism of the photo-reaction will be proposed.

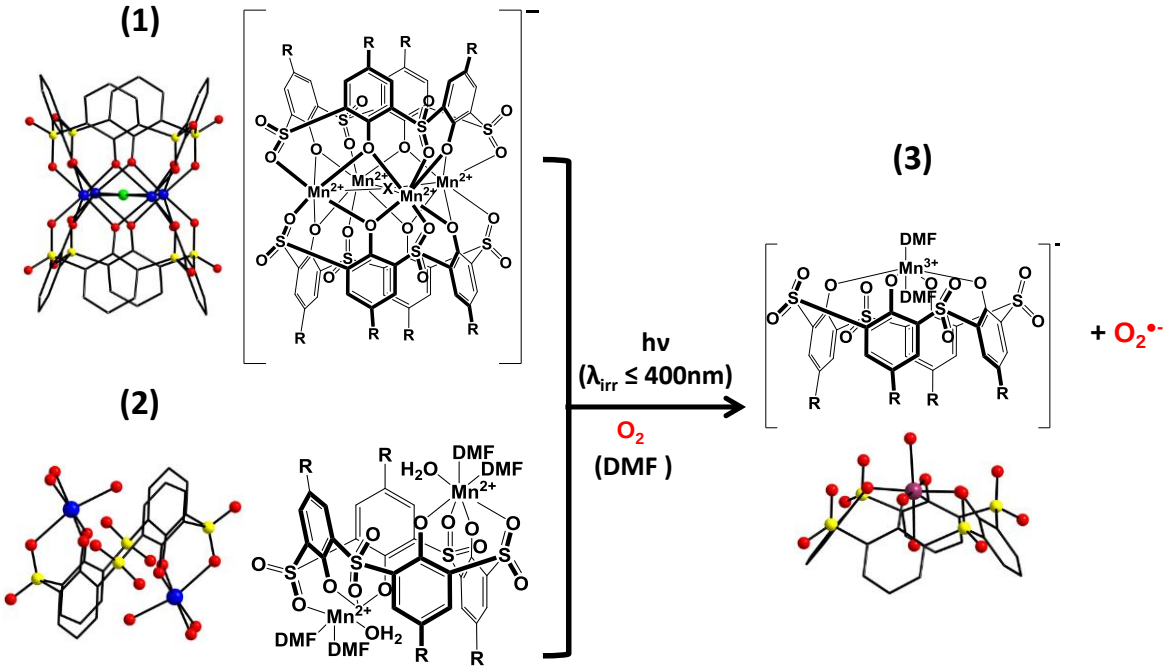

Scheme 1. Photo-reactivity of compounds 1 and 2. R = *tert*-butyl or H. Each atom is depicted as follows: Mn^{2+}, blue; Mn^{3+}, violet; S, yellow; O, red.

Results and Discussion

Compounds 1 and 2 (R= *tert*-butyl) were prepared by using the methods described in the literature.[6],[7],[8] Compound 1 is composed of squares of four manganese(II) ions sandwiched between two $ThiaSO_2$ macrocycles in cone conformation. In the middle of the square formed by the four manganese(II) ions, the presence of μ_4-F gives a negative charge to the cluster. The electroneutrality of the complex is achieved by the presence of the K^+ cation, coordinated by sulphonyl and methanol groups (Scheme 1). The structure of this aggregate, with a sevenfold $[MnO_6F]$ coordination polyhedron having approximately C_{2v} symmetry, has already been discussed in a previous article [5, 6]. Compound 2 is composed of two manganeses(II) ions with a sixfold $[MnO_6]$ coordination polyhedron having approximately O_h symmetry, and the macrocycle is in 1,2 alternate conformation (Scheme 1).

Photo-physical characterisation of compound 2 in DMF. Figure 1 shows the absorption, emission and excitation spectra of 2 at room temperature in DMF. For absorption, two bands maxima are observed at 28410 cm^{-1} (352 nm) and 34965 cm^{-1} (286 nm), respectively. These absorption bands are the signature of the $ThiaSO_2$ calixarene ligand and correspond to $n\rightarrow\pi^*$ and $\pi\rightarrow\pi^*$ transitions, respectively. The molar extinction coefficient (ε_{max}) of the intense absorption band of the dinuclear complex at 28410 cm^{-1} is equal to 47200 $M^{-1}cm^{-1}$, which is approximately 65% of the compound 1 (ε_{max} = 72000 $M^{-1}cm^{-1}$) studied previously.[6]

The emission spectrum of 2 in DMF solution upon photoexcitation at 28570 cm^{-1} (350 nm) exhibits a broad luminescence band between 12000 and 18000 cm^{-1} (555 - 833 nm) with a maximum centred at 14350 cm^{-1} (697 nm). This red luminescence with a very large gap between the strong absorption at 28410 cm^{-1} and the broad emission at 14350 cm^{-1} (ΔE = 14060 cm^{-1}), comes from the lowest energy component of the $^4T_1(t_{2g}^4e_g^1) \rightarrow {}^6A_1(t_{2g}^3e_g^2)$ d-d transition of the Mn^{II} ions in d^5 high-spin configuration.

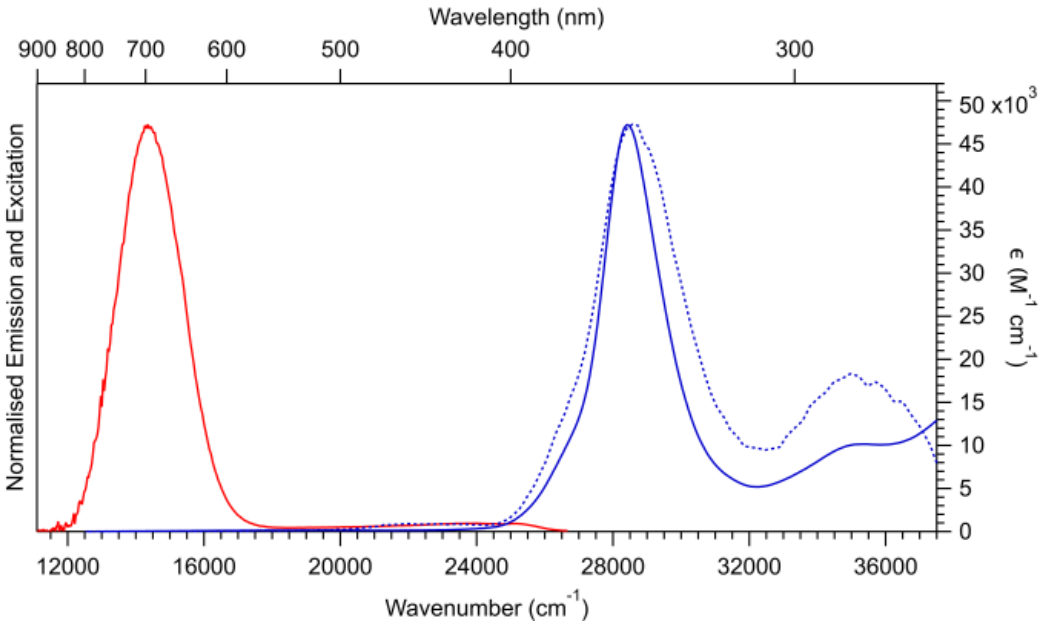

Figure 1. Absorption (blue curve), excitation (blue dotted curve) and emission (red curve) spectra in DMF solution of $[(ThiaSO_2)(Mn^{II})_2(DMF)_4(H_2O)_2]$ 2 at room-temperature, c = 1.54 x 10^{-5} M.

The crystal structure for 2 [8] reveals a pseudo octahedral coordination sphere for the Mn^{II} ions, resulting is a large splitting of the $^4T_1$ state of octahedral parentage. This geometry is quite different from the one in tetra-nuclear complex in which the Mn^{II} ions show a sevenfold coordination sphere and a monocapped trigonal prismatic geometry close to C_{2v} symmetry.[6] So, photoexcitation at 28570 cm^{-1} (350 nm) into the ligand centred n→π*/π-π* transitions is followed by fast intersystem crossing and internal conversion, thus resulting in the relatively intense red metal-centred dd luminescence.

The excitation spectrum of compound 2 in DMF solution was collected at the emission band maximum, the spectrum measured is indeed perfectly superimposed to the absorption spectrum thus proving unambiguously that the emission is intrinsic to the complexes. The concentration used for the excitation (c = 1.54 x 10^{-5} M) is low in order to minimise saturation effects in the region of the strong UV absorption bands.

O_2 pressure-dependence of the manganese(II) luminescence-quenching in solution. The presence of oxygen in the DMF solution quenches the Mn^{II} luminescence. In solution, the $[(ThiaSO_2)(Mn^{II})_2(DMF)_4(H_2O)_2]$ entities are considered as totally isolated. The luminescence spectra of solution of 2 after different times (0 – 300 s) of de-oxygenation by N_2 bubbling were shown in Figure 2. The maximum luminescence intensities are observed after only 80 s of N_2 bubbling. The phenomenon is reversible as function of time (0 – 4500 s) of re-oxygenation of the N_2 saturated solution by exposing it to air (see Figure S5). The luminescence intensity increases and decreases by N_2 bubbling (de-oxygenation) and by exposing to air (re-oxygenation), respectively. The quenching of the spin-forbidden Mn^{II} centered $^4T_1 \rightarrow {}^6A_1$ luminescence is given by a spin-conserving energy transfer process from the excited complex to O_2 thereby exciting O_2 from its $^3\Sigma^-_g$ ground state to the $^1\Sigma^+_g$ excited state.[9]

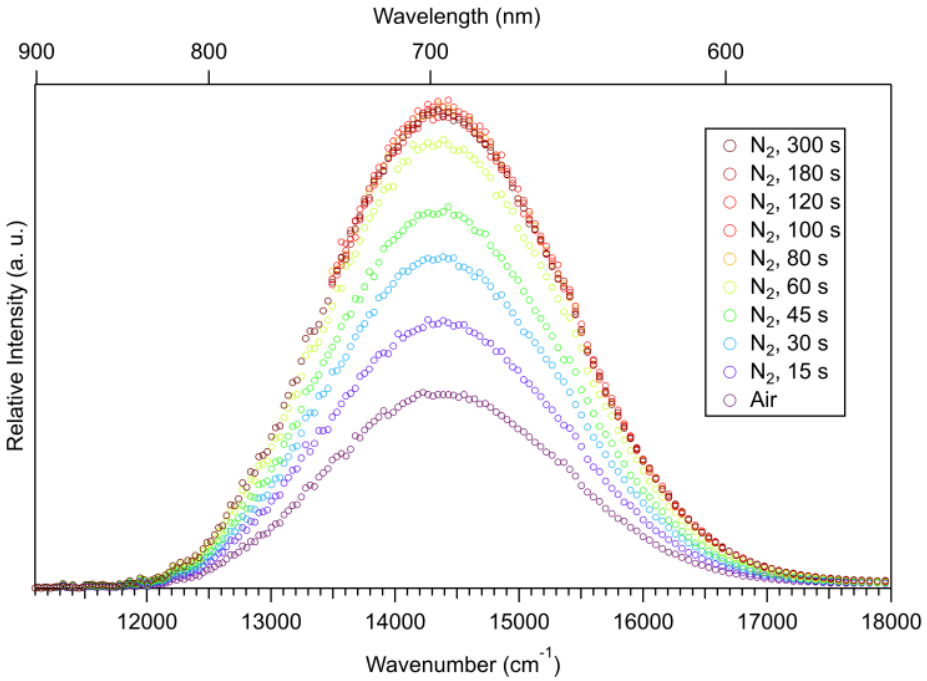

Figure 2. Solution emission spectra of $[(ThiaSO_2)(Mn^{II})_2(DMF)_4(H_2O)_2]$ 2 after different times (0 – 300 s) of de-oxygenation by N_2 bubbling and upon photoexcitation at 28570 cm^{-1} (350 nm).

Solid-state emission, excitation, temperature-dependence and O_2 pressure-dependence of the Mn^{II} luminescence. The solid-state emission and excitation spectra for 2 are shown in Figure S6. The compound 2 exhibits an intense broad emission band centred at 15200 cm^{-1} (658 nm) with a full width at half maximum (FWHM) of about 2200 cm^{-1} upon photo-excitation at 28570 cm^{-1} (350 nm). As in solution, the luminescence emission comes from the $^4T_1(t_{2g}{}^4e_g{}^1) \rightarrow {}^6A_1(t_{2g}{}^3e_g{}^2)$ transition of the Mn(II) ions in d^5 high-spin configuration. The solid-state excitation spectrum of 2 shows a saturated UV region (above 23000 cm^{-1}) from the ligand-centred absorption bands. On the other hand, at lower energy, the excitation spectrum presents a broad and structured band with two maxima at about 17900 cm^{-1} (559 nm) and 19100 cm^{-1} (524 nm), respectively. The two maxima can be assigned to the split components of the d-d $^4T_1 \rightarrow {}^6A_1$ transition of Mn^{II}.

The emission of 2 in the solid-state at variable temperature (8.5 - 300 K) and in vacuum (to avoid the quenching by O_2) under excitation at 28570 cm^{-1} (350 nm) is shown in Figure S7. The orange-red luminescence decreases between 8.5 and 300 K. The FWHM increases continuously by 23% over the whole temperature range from 2200 to 2700 cm^{-1}, as shown in Figure S8. The emission maximum $\overline{\nu}_{max}$ shifts to lower energies between 8.5 and 100 K, to reach a minimum of 15000 cm^{-1} then shifts to slightly higher energies above 100 K (Figure S8).

The luminescence lifetime for 2 under a photo-excitation at 28170 cm^{-1} (355 nm) between 3 K and 293 K are included in Figure S9. The decay curves calculated by Igor fitting software varied from 485 μs at 3 K to 114 μs at 293 K.[10] Compared to the tetra-nuclear complexes, the luminescence lifetimes for 2 are five time lower at low temperature (τ = 2.12 - 2.31 ms).[6]

As in solution, the Mn^{II} luminescence in the solid-state is quenched by the presence of oxygen. Figure S10 shows the luminescence intensity decreasing as function of the air pressure between 0.1 and 1010 mbar at room-temperature. The behaviour observed is

reversible and reproducible as in solution, and as for the tetra-nuclear complexes previously studied.[7] The luminescence intensities of Mn^{II} evolve positively or negatively by removing from or introducing O_2 into sample compartment.

Crystal structure of $[(ThiaSO_2)(Mn^{III})(DMF)_2]Na$ 3

The preparation and crystals structures of the tetranuclear complex 1 and the dinuclear complex 2 are described in previous works.[5,6,8] The mononuclear complex 3 is obtained by illumination at 400 nm of complex 1 in DMF solution. By adding $NaNO_3$ salt, 3 crystallises from 1 (R=H) in DMF (0.01 M) in the form of violet platelets in the orthorhombic space group *Pbca* (n°61) (see Figures S11, S12 and crystallography tables in supporting information). If the illumination of solution 1 is not sufficiently prolonged, crystals of 2 and 3 can be obtained together. The formation of 3 from 1 can either result in two complexes of 3 or a complex of 3 and a complex of 2. Compound 3 consists of $[(ThiaSO_2)(Mn^{III})(DMF)_2]^-$ anions whose charge is compensated by the presence of the Na^+ cations, coordinated by phenolate, sulfonyl and DMF oxygen and inducing the formation of chain in the solid state. The negative charge of the $[(ThiaSO_2)(Mn^{III})(DMF)_2]^-$ complex indicates that the four phenol groups of $ThiaSO_2$ are deprotonated and that the charge of the manganese ion is +3.

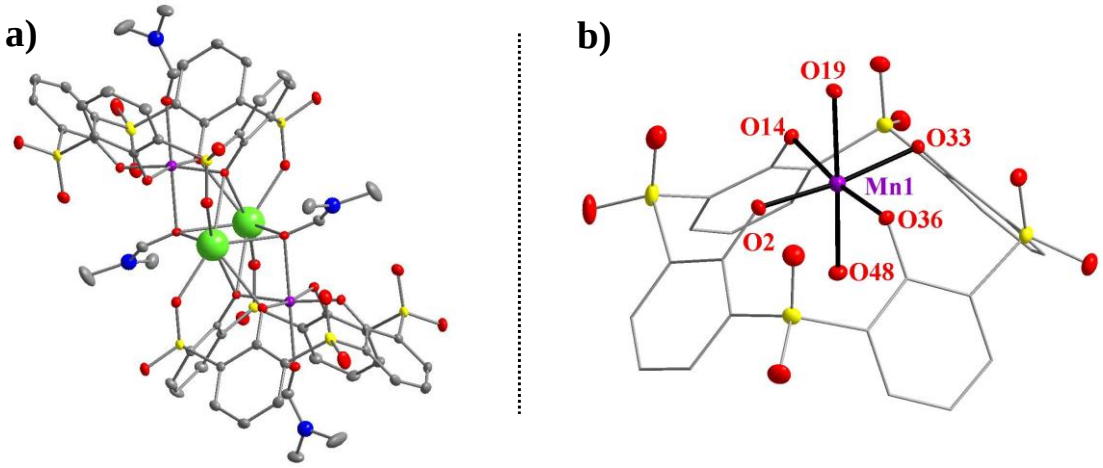

Figure 3. Structures arise from an analysis of single crystal X-ray diffraction data (for details see Supporting Information). Two views of compound 3: a) Ball and stick representation. Each atom is depicted as follows: Mn, violet; S, yellow; O, red; C, grey; N, blue; Na, Green. Hydrogen atoms are omitted for clarity. b) Representation of the octahedral coordination of Mn^{3+}.

The manganese ion is in axial distorted octahedral coordination geometry (Figure 3) with the Jahn-Teller axes defined by O19(DMF)-Mn-O48(DMF), which is commonly observed for high spin d^4 transition metal ions (d_{Mn-O19} = 2.22 Å; d_{Mn-O48} = 2.17 Å; d_{Mn-O2} = 1.89 Å; d_{Mn-O14} = 1.92 Å; d_{Mn-O33} = 1.95 Å; d_{Mn-O36} = 1.92 Å). The Mn^{III} ion position, between the four phenolate oxygen, is common for calix[4]arene macrocycle. One example has been already observed for a mononuclear complex[11] and several examples for polynuclear complex formed with mixture of Mn^{III}/Mn^{II}[12],[13] or Mn^{III}/Ln^{III}.[[14]] For the Thiacalixarene family, where the presence of the S, SO or SO_2 bridges of calix rims has the effect to push the metal ions away from the centre of the tetra-phenolic chelate, this coordination mode is not common.

Photo-reactivity of compounds 1 and 2 in solution

Irradiation of colourless solutions of 1 or 2 in quartz cells at 20 °C with a light diode (400 nm, nominal flux of 586 mW/cm^2 at a working distance between the source and the sample of d = 10 mm) under an ambient air atmosphere resulted in the rapid conversion of the colourless solutions of 1 and 2 to violet solutions. Monitoring this reaction by UV-vis spectroscopy (Figure 4) revealed the quantitative conversion of initial complexes (λ_{max} = 350 nm for 1 and 355 nm for 2) to 3 (λ_{max} = 347, 540 nm for 1 and λ_{max} = 338, 530 nm for 2). Continued irradiation at 400 nm of the reaction mixture after the appearance of the final spectrum did not lead to any further changes in the UV-vis profile, indicating that the anion 3 is the final product of these reactions. Irradiation was also carried out at two different wavelengths, one at 365 nm centred on the maximum absorption of the ThiaSO_2 ligand (π - π^*) (see Figure S1 and S2) and one at 465 nm, which is outside the limits of absorption of the two complexes.

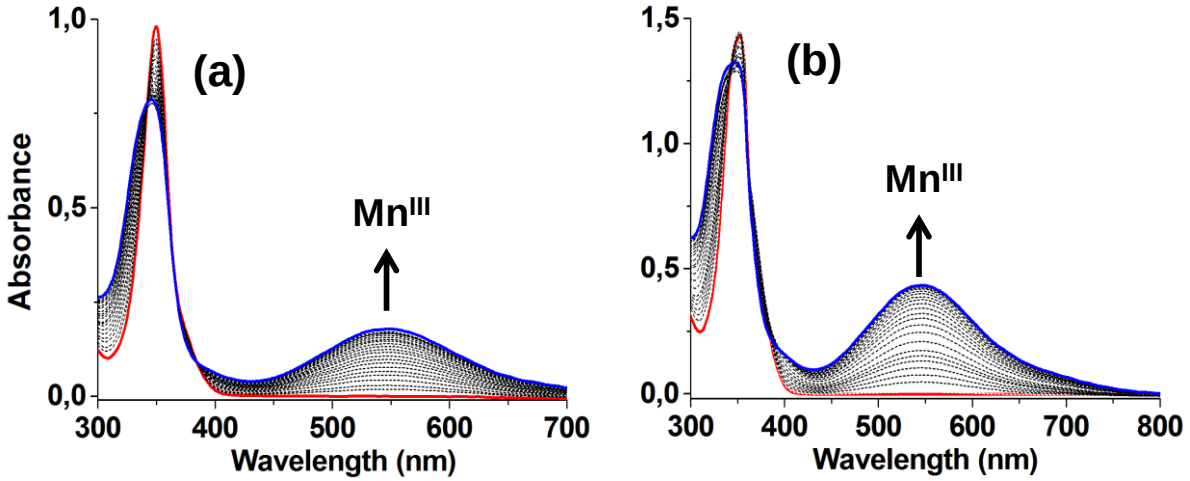

Figure 4. Time-resolved UV-vis spectral changes observed during irradiation at 400 nm of aerobic solutions in DMF at 20 °C of (a) 1 from 0 - 70 min, c = 30 µM, d = 0.5 cm, and ((b) 2 from 0 – 34 min, c = 300 µM, d = 0.2 cm.

At 365 nm, irradiation of 1 leads to a much faster reaction than at 400 nm, whereas for the solution of 2 the reaction time is more or less identical for either wavelength. This observation may indicate that the limiting step in the case of the transformation of 2 could be the change in conformation of the macro-cycle required to obtain 3. No reaction is observed under irradiation at 465 nm for either complex. For both 1 and 2 no reaction are observed in the absence of light, whether at room temperature or higher temperatures (100°C). In the absence of O_2 (under vacuum or inert atmosphere), illumination leads to no transformation. These observations confirm the effective photo-reactivity phenomena existing between the ThiaSO$_2$/Mn^{II} system and oxygen.

The oxidation state of manganese ion has been confirmed in 3 by electronic paramagnetic resonance spectroscopy. Figure 5 shows the parallel mode EPR spectrum of 3 in frozen solution and simulation (green curve) which have parameters as follows: S = 2, g = [2, 1.99, 1.985], D = 2.17 cm^{-1}, E/D = 0.11, a = [60.7, 60.7, 58.9] G and Dpa = 2°. This signal (blue curve) is centred at an effective g value of 8.2 and consists of six hyperfine lines separated by a_{av}=60.1G..These values are compatible with an Mn^{III} signature.[15][16] Figure S3 shows the

effect of a temperature increase on its EPR intensity. Above 25 K it decreases rapidly as expected for a non-Kramers ion. However, Figure S4 shows a characteristic spectrum of Mn^{II}[16] ion in the S = 1/2 state with hyperfine interactions (I = 5/2) and forbidden transitions (IΔMiI = 1) 3, g_{av} ~ 2.01, a_{av} ~ 93.4 G. This EPR signal reveals that when complex 1 or 2 was illuminated in this experiment, only part of the Mn^{II} was oxidized to Mn^{III}.

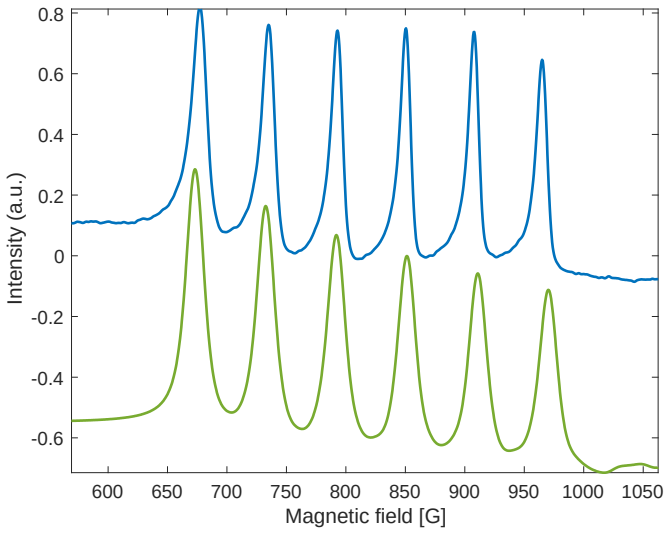

Figure 5. Parallel mode - EPR spectrum (blue curve) of 3 at T = 11 K. Green curve is the simulation of the experimental data.

The necessary presence of oxygen for this reaction and the resulting Mn^{III} ion in the final complex suggest a mono-electronic exchange between the Mn^{II} ions and oxygen during the reaction, and thus the production of the superoxide ion. In order to confirm this, EPR spectroscopy in the presence of 5,5-Dimethyl-1-pyrroline N-oxide (DMPO) was carried out. Preliminary irradiation tests at 400 nm in the presence of DMPO with and without the manganese complexes showed that DMPO is sensitive to illumination in the presence of oxygen without the complexes. This is why the DMPO was added just after the illumination of the complex solution. The spectrum obtained (Figure 6) shows the signature of DMPO-OOH,[17] simulated with following values: S = 1/2, g = 2.006, a_N = 13.2 G,

$a_{Hß}$ = 9.3 G, a_{Hr} = 1.8 G and supports the hypothesis that during illumination the superoxide ion is generated. An example of a mononuclear complex with zwitterionic calix[4]arene displays a linear end on Mn^{III}-O_2 arrangement obtained by reacting the calixarene macrocycle with O_2 and manganese(II) acetate. [18]. The redox reaction of our system appears to be similar but in our case we were never able to isolate the coordinated superoxide group on complex 3.

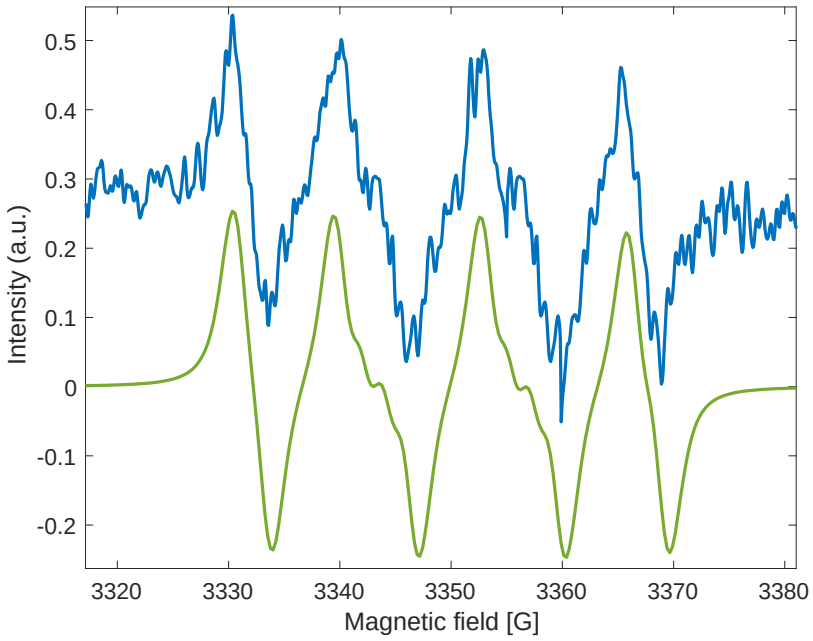

Figure 6. EPR spectrum (blue curve) of 1 solution in DMF illuminated at 400 nm and RT. Green curve is the simulation of the experimental data.

The luminescence of 1 and 2 is quenched, in the solid state and in solution, by an energy transfer with oxygen leading to the formation to the singlet oxygen from triplet oxygen. In solution, the transformation of complexes 1 and 2 into complex 3 is achieved by electron transfer between the complexes and oxygen. Thus, the quenching, by oxygen, of systems 1 and 2, can occur according to two mechanisms: type I, due to photo-induced electron transfer and type II, caused by energy transfer from triplet state of the photosensitizer. These mechanisms can often take place successively (Scheme 2).

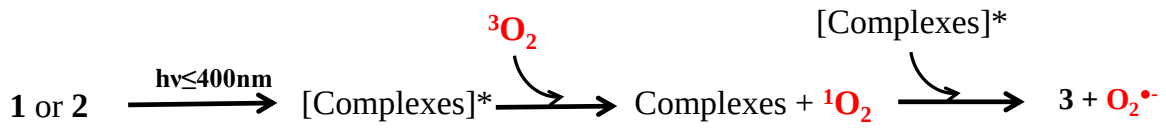

Scheme 2. Photo-reactivity of compounds 1 and 2.

When 1 or 2 are illuminated in DMF solution in the presence of triphenylphosphine, the formation of compound 3 occurs when all triphenylphospine has been converted to triphenylphosphine oxide (reaction followed by GCMS). Thus, for these systems, the photo-oxidation mechanism seems to start with an energy transfer (production of singlet oxygen), then ends with an electron transfer between the complex and thus-created singlet oxygen leading to the formation of compound 3 and the superoxide ion. The presence of singlet oxygen in this case seems to be essential.

Conclusions

Thiacalixarene complexes have been studied since the late 1990's for their magnetic, electronic and optical properties, with various potential applications such as molecular recognition, catalysis, self-assembly (porous materials) and nanomedicine. The thiacalixarene complex $[(ThiaSO_2)(Mn^{II})_2(DMF)_4(H_2O)_2]$ 2 has been characterised by luminescence studies and presents an intense and broad luminescence band similarly to the thiacalixarene complex $[(ThiaSO_2)_2(Mn^{II})_4F]K$ 1, which has been previously characterised and reported. The fact that both of these complexes display luminescence behaviour illustrates that neither the coordination of the Mn^{II} ions, nor the conformation of the macrocycle, have any influence over the occurrence of this phenomenon. The presence of oxygen, both in solution and in the solid state, quenches the Mn^{II} luminescence by energy transfer from the excited complex to O_2 thereby exciting O_2 from its $^3\Sigma^-_g$ ground state to the excited $^1\Sigma^+_g$ state. The conversion of complexes 1 and 2 to the mononuclear complex 3, by illumination and via reaction with O_2,

has been demonstrated. To our knowledge, this transformation was heretofore unknown for the transformation of an Mn^{II} ion to an Mn^{III} ion solely coordinated by oxygen. The hypothetical photo-oxidation mechanism, for this type of reaction of these compounds, is first of all a type II energy transfer followed by a type I electron transfer. This work marks the remarkable capacity of $ThiaSO_2$ to act as an antenna for the Mn^{II} ion. The ability to photo-oxidize Mn^{II} ions in solution and the multitude of functionalization possibilities on the thiacalixarene macrocycle open up a many prospective areas of interest.

Experimental Section

All chemicals and solvents were used as received (solvents and chemicals: Aldrich); The ligands, p-tertbutylthiacalix[4]arene (ThiaS),[19] p-tert-butylsulphonylcalix-[4]arene ($ThiaSO_2$)[20] and compound[5] and 2[8] were synthesised by the published procedures. For illumination experiments, LEDs of various wavelengths 360 and 400 nm were used. The LED were purchased from LED ENGINE Co and calibrated with a flame spectrometer from Ocean Optic with a nominal flux of 430 and 586 mW/cm^2 respectively, at a working distance between the source and the sample of d = 10 mm.

Single Crystal X-Ray Diffraction XRD. Suitable crystals were selected and mounted on an Xcalibur kappa-geometry diffractometer (Rigaku OD, 2015) equipped with an Atlas CCD detector and using Mo radiation ($\lambda = 0.71073$ Å). Intensities were collected at 150 K by means of the CrysalisPro[21] software. Reflection indexing, unit-cell parameters refinement, Lorentz-polarisation correction, peak integration and background determination were carried out with the CrysalisPro software. An analytical absorption correction was applied using the modeled faces of the crystal.[22] The structures were solved by direct methods with SIR97[23] and the least-square refinement on F^2 was achieved with the CRYSTALIS software.[24] All non-hydrogen atoms were refined anisotropically. The hydrogen atoms were all located in a

difference map, but those attached to carbon atoms were repositioned geometrically. The H atoms were initially refined with soft restraints on the bond lengths and angles to regularise their geometry (C-H in the range 0.93 - 0.98 Å, and Uiso(H) in the range 1.2 - 1.5 times Ueq of the parent atom), after which the positions were refined with riding constraints. For the experimental details see supporting information. CCDC-1854716 contains the supplementary crystallographic data for this paper. These may be obtained free of charge from The Cambridge Crystallographic Data Centre via www.ccdc.cam.ac.uk/data_request/cif.

EPR spectroscopy.

EPR experiments were performed with a Bruker X band spectrometer EMX plus, double mode for Mn samples and E500, with a standard cavity for DMPO sample. Microwave powers of 2-13 mW, modulation amplitude 4-5 G and field modulation 100 kHz were used. The simulations were realized with easyspin (Matlab tools).

Spectroscopic Measurements. Electronic absorption, excitation and emission spectra in the UV-Vis-near IR were recorded at 293 K from solutions in dimethylformamide (DMF) and in the solid-state with a double beam absorption spectrometer (Agilent, Cary 5000) and a commercial fluorimeter (Jobin Yvon Horiba FL3-22, Fluorolog-3) equipped with a Peltier-cooled photomultiplier (Hamamatsu R2658P, sensitivity: 185 - 1010 nm) using quartz cells of 0.2 cm and 1 cm path length, for the absorption, and excitation-emission spectra, respectively. Powder samples were mounted directly onto copper plates using conductive silver glue and cooled in an optical closed-cycle cryostat capable of reaching temperatures down to 3 K in a helium atmosphere (Sumitono SHI-950/Janis Research CCS-500/204). High resolution emission spectra were recorded upon excitation with 405 nm diode lasers or with a Nd:YAG laser (Quantel Brillant B) using the third harmonic at 355 nm. The emitted light was analysed at 90° with a Spex 270M monochromator with holographic gratings (150 grooves/mm, blazed

at 600 nm). Light intensities were detected by a photomultiplier (Hamamatsu R928) or CCD camera. Appropriate filters were utilised to remove the laser light, the Rayleigh scattered light and associated harmonics from the emission spectra. The emission spectra were corrected for the instrumental response function. Luminescent lifetimes were measured using the excitation provided by a the third harmonic of the Nd:YAG. The output signal of the photomultiplier was fed into a multichannel scaler (Stanford Research SR-400) and transferred to a PC for data analysis. Lifetimes were averages of 3 independent determinations. The air pressure-dependent solid-state luminescence spectra have been realised in a cryostat equipped with a primary pump and an APG100 active Pirani vacuum gauge (Edwards).

Acknowledgements

Support for EPR measurements was provided by the fédération RENARD and the Departement de Chimie Moléculaire, Université Grenoble Alpes.

[1] Suppan, P. Chemistry and Light; The Royal Society of Chemistry:Cambridge, U.K., 1994.
[2] Kavarnos George J. Fundamentals of photoinduced electron transfer; VCH Publishers, 1993.
[3] Maria C. DeRosa, Robert J. Crutchley, Coord. Chem. Rev., 2002, 233/234,pp 351-371
[4] Dana M. Wagnerová, Kamil Lang, Coord. Chem. Rev., 2011, 255, 2904– 2911.
[5] Lamouchi, M., Jeanneau, E., Pillonnet, A., Brioude, A., Martini, M., Stephan, O., Meganem, F., Novitchi, G., Luneau, D., Desroches, C., Dalton Trans., 2012, 41(9), 2707-2713.
[6] Suffren Y., O'Toole N., Hauser A., Jeanneau E., Brioude A., Desroches C., Dalton Trans., 2015, 44, 7991–8000.
[7] T.Kajiwara, S.Yokozawa, T.Ito, N.Iki, N.Morohashi, S.Miyano, Chem. Lett., 2001,6.
[8] R.O.Fuller, G.A.Koutsantonis, Ivan Lozic, M.I.Ogden, B.W.Skelton, Dalton Trans., 2015, 44, 2132-2135.
[9] (a) R. Q. Albuquerque, Z. Popovic, C. L. De, G. Calzaferri, ChemPhysChem, 2006, 7, 1050–1053; (b) M. S. Khakhalina, O. A. Rodionova, M. V. Puzyk, Opt. Spectrosc., 2009, 106, 529–531; (c) M. V. Mina, M. V. Puzyk, Opt. Spectrosc., 2011, 111, 71–73; (d) C. A. Kent, D. Liu, A. Ito, T. Zhang, M. K. Brennaman, T. J. Meyer, W. Lin, J. Mater. Chem. A, 2013, 1, 14982–14989.
[10] IGOR PRO v. 6.36, Wavemetrics Inc., Oregon.
[11] Lei-Lei Liu, Hong-Xi Li, Li-Min Wan, Zhi-Gang Ren, Hui-Fang Wang, Jian-Ping Lang, Chem.Commun., 2011, 47, 11146.
[12] R.McLellan, M.A. Palacios, S. Sanz, E.K. Brechin, S.J.Dalgarno, Inorg.Chem., 2017,56,10044.
[13] S.M. Taylor, R.D. McIntosh, S. Piligkos, S.J. Dalgarno, E.K. Brechin, Chem.Commun., 2012, 48, 11190.
[14] M.A. Palacios, R. McLellan, C.M. Beavers, S.J. Teat, Hgni Weihe, S. Piligkos, S.J. Dalgarno, E.K. Brechin, Chem.-Eur.J., 2015, 21, 11212.

[15] K. A. Campbell, E. Yikilmaz, C. V. Grant, W. Gregor, A.-F. Miller, R. D. Britt, J. Am. Chem. Soc. 1999, 121, 4714-4715.
[16] G. Brouet, X. Chen, C. Wee Lee, L. Kevan, J. Am. Chem. Soc. 1992,114, 3720-3726
[17] a) G. R. Bueyrner, Free Radical Biology & Medicine, Vol. 3, pp. 259-303, 1987; b) Nosaka, Y., Nosaka, Y., Chem.Rev.,2017, 117, 11302.
[18] L. Lei-Lei, L. Hong-Xi, W. Li-Min, R. Zhi-Gang, W. Hui-Fang, L. Jian-Ping, Chem. Commun., 2011, 47, 11146.
[19] (a) Kumagai, H.; Hasegawa, M.; Miyanari, S.; Sugawa, Y.; Sato, Y.; Hori, T.; Ueda, S.;Kamiyama, H.; Miyano, S. Tetrahedron Lett., 1997, 8, 3971-3972. (b) Iki, N.; Kumagai, H.; Morohashi, N.; Ejima, K.; Hasegawa, M.; Miyanari, S.; Miyano, S., Tetrahedron Lett., 1998, 39, 7559.
[20] (a) Mislin, G.; Graf, E.; Hosseini, M. W.; Bilyk, A.; Hall, A. K.; Harrowfield, J. M.; Skelton, B. W.; White, A. H., J. Chem. Soc., Chem. Commun 1999, 373-374. (b) Morohashi, N.; Narumi, F.; Iki, N.; Hattori, T.; Miyano, S., Chem.Rev., 2006, 106, 5291.
[21] Rigaku Oxford Diffraction, (2018), CrysAlisPro Software system, version 1.171.xx.xx, Rigaku Corporation, Oxford, UK.
[22] Clark, R. C. & Reid, J. S. (1995). Acta Cryst. A51, 887-897.
[23] Altomare, A.; Burla, M.C.; Camalli, M.; Cascarano, G. L.; Giacovazzo, C.; Guagliardi, A.; Grazia, A.; Moliterni, G.; Polidori, G.; Spagna, R. J. App. Cryst. 1999, 32, 115-119.
[24] Betteridge, P.W.; Carruthers, J. R.; Cooper, R. I.; Prout, K.; Watkin, D. J., J. Appl. Cryst.2003, 36, 1487.